Altered Small-World Anatomical Networks in Apolipoprotein-E4 (ApoE4) Carriers using MRI

Mohammed Goryawala [1], Qi Zhou [1], Ranjan Duara [3], David Loewenstein [2], Mercedes Cabrerizo[1], Warren Barker [3], Malek Adjouadi [1]

Abstract— **Apolipoprotein E (ApoE) gene and primarily its allele e4 have been identified as a risk factor for Alzheimer's disease (AD). The prevalence of the gene in 25-30% in the population makes it essential to estimate its role in neuroregulation and its impact on distributed brain networks. In this study, we provide computational neuroanatomy based interpretation of large-scale and small-world cortical networks in cognitive normal (CN) subjects with differing Apolipoprotein-E4 (ApoE4) gene expression. We estimated large-scale anatomical networks from cortical thickness measurements derived from magnetic resonance imaging in 147 CN subjects explored in relation to ApoE4 genotype (e4+ carriers (n=41) versus e4- non-carriers (n=106)). Brain networks were constructed by thresholding cortical thickness correlation matrices of 68 bilateral regions of the brain analyzed using well-established graph theoretical approaches. Compared to ApoE4 non-carriers, carriers showed increased interregional correlation coefficients in regions like precentral, superior frontal and inferior temporal regions. Interestingly most of the altered connections were intra-hemispheric limited primarily to the right hemisphere. Furthermore, ApoE4 carriers demonstrated abnormal small-world architecture in the cortical networks with increased clustering coefficient and path lengths as compared to non-carrier, suggesting a less optimal topological organization. Additionally non-carriers demonstrated higher betweenness in regions such as middle temporal, para-hippocampal gyrus, posterior cingulate and insula of the default mode network (DMN), also seen in subjects with AD and mild cognitive impairment (MCI). The results suggest that the complex morphological cortical connectivity patterns are altered in ApoE4 carriers as compared to non-carriers, providing evidence for disruption of integrity in large-scale anatomical brain networks.**

I. INTRODUCTION

Brain networks have been widely studied using functional brain data including electroencephalogram (EEG)[1], magneto-encephalogram (MEG)[2], and functional Magnetic Resonance Imaging (fMRI)[3]. Also, rest-state fMRI and diffusion tensor imaging (DTI)[4] have been recently explored as a means to explore the complex pattern of human brain connections under rest. Recent studies have developed small-world connectivity networks based on structural imaging characteristics such as regional cortical thickness and cortical volumes to explore the influence of AD on small-world characteristics[5].

ApoE4 genotype has been postulated to be a major risk factor for developing AD or for progression to AD from MCI. ApoE4 carriers have shown to display increased plaque deposition and increased temporal lobe atrophy [6]. Also, ApoE4 carriers seem to have greater impairment in episodic memory, and also hippocampal atrophy well correlated with reduced memory performance, which is not seen in non-carriers. Also, since ApoE4 carriers show increased amyloid beta (Aβ) in the cortex, it is postulated that E4 carriers show increased cortical dysfunction. Findings by Wolk et al. suggest a differential impact of the disease in carriers vs. non-carriers [6].

Small-world connectivity networks serve as important tools to study the brain's complex networks not only for visualizing the networks but for providing quantitative assessments of the relevant network parameters [7]. Small-world connectivity measures have shown increased clustering coefficient and the longest absolute path length in AD and MCI subjects as compared to controls postulating a less optimal organization of the cortical networks[5].

In the present study, we evaluated cortical networks created using cortical thickness produced by FreeSurfer[8] using MRI scans for 147 cognitively normal (CN) subjects as a function of the ApoE4 genotype to understand the role and impact of genetic factors on large scale networks of the brain. We aim to understand the changes in the small world connectivity parameters of carriers of ApoE4 versus non-carriers to visualize and quantify any changes in structural connectivity networks of the brain. The hypothesis behind this study is that ApoE4 carriers may display a different pattern of connections in their cortical networks independent of the disease.

II. MATERIALS AND METHODS

A. Study Data

Data used in this study were obtained from the Alzheimer's Disease Neuroimaging Initiative (ADNI) database (adni.loni.usc.edu). Baseline volumetric MRI data for 147 cognitively normal (CN) subjects explored in relation to Apolipoprotein E type allele (ApoE4) genotype (e4+ (n=41) versus e4- (n=106)). Cognitively Normal Subjects (CN) individuals with MMSE scores between 24 and 30 (inclusive), a CDR of 0, non-depressed, non-MCI, and non-demented were included in the study.

B. Imaging Protocol

MRI scans were acquired from a variety of 3T scanners with protocols individualized for each scanner, as defined at (http://adni.loni.usc.edu/methods/documents/mri-protocols/).

Research is supported through NSF grants CNS-0959985, CNS-1042341, HRD-0833093, IIP 1338922 and IIP-1230661.

M. Goryawala, Q. Zhou, M. Cabrerizo, and M. Adjouadi* are with the Department of Electrical Engineering at Florida International University, Miami FL 33174 USA (email: qzhou003@fiu.edu; mgory001@fiu.edu; cabreriz@fiu.edu; jwang006@fiu.edu and adjouadi@fiu.edu).

W. Barker, D. A. Loewenstein and R. Duara are with the Wien Center for Alzheimer's Disease and Memory Disorders, Mount Sinai Medical Center, Miami Beach, FL 33140 USA (email: warren.barker@msmc.com; DLoewenstein@med.miami.edu; ranjan.duara@msmc.com). *Asterisk indicates corresponding author.*

C. MRI Image Analysis

FreeSurfer pipeline (version 5.1.0) was applied to the MRI scans to produce mean cortical thickness maps in the Desikan-Killiany atlas resulting in 34 regional thicknesses for each hemisphere and a total of 68 cortical thickness parameters for each subject as shown in Figure 1 A and B. The regional cortical thicknesses were corrected for age, gender, age-gender interaction and mean overall cortical thickness using linear regression. The residuals of the regression were substituted instead of the raw mean cortical thicknesses for the connectivity analysis.

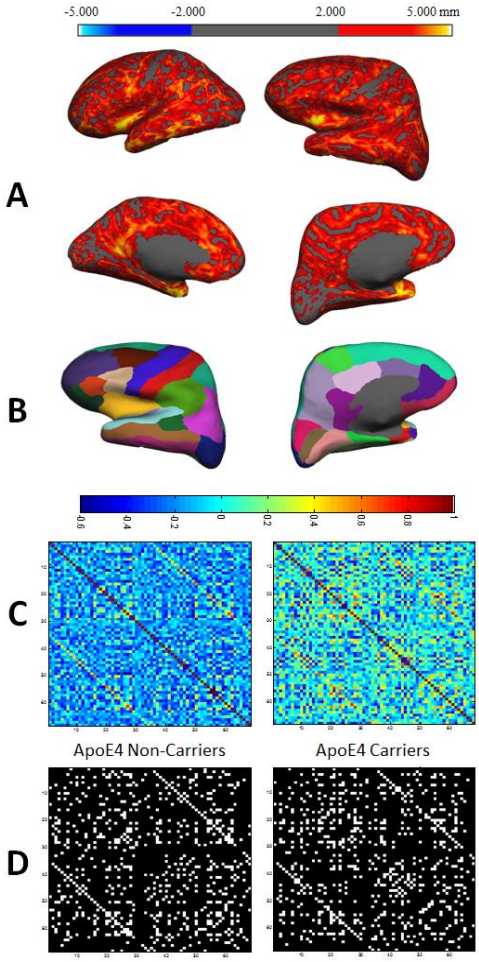

Figure 1. Construction of structural cortical networks. **A.** Two representative cortical thickness maps for ApoE4 non-carriers (left) and ApoE4 carriers (right) obtained from FreeSurfer from MRI. **B.** Segmentation of the entire cerebral cortex in 68 regions **C.** Cortical ACMs for each group (left: ApoE4 non-carriers and right: ApoE4 carriers) **D.** Binarized ACMs at threshold of 30% sparsity.

D. Constructing Cortical Anatomical Connectivity Matrix

Anatomic Connectivity Matrix (*ACM*) are defined as statistically significant correlations within regions of the anatomical framework of the brain as measures through pairwise correlations using the mean cortical thickness of a brain region. Cortical *ACM* P_{ij} (i=1...N; j=1...N, N=68), for each group was constructed by calculating the Pearson correlation coefficient across individuals by using the mean cortical thickness of each pair of regions as shown in Figure 1 C. The 68x68 ACMs constructed for each group were binarized using a fixed threshold.

$$P_{ij} = cov(MCT_i\ ,\ MCT_j)/\sigma_i\sigma_j \quad (1)$$

where, $cov(MCT_i\ ,\ MCT_j)$ is the covariance between mean cortical thickness of region i and region j and σ_i and σ_j are the respective standard deviations. Further, the ACM is binarized such that,

$$if\ P_{ij}\ \geq\ \theta\ then\ A_{ij} = 1, else\ \ A_{ij} = 0 \quad (2)$$

where, θ is the sparsity threshold as discussed in the next section. The binarized *ACM (A),* as shown in Figure 1 *D,* display an underlying topological connection between different regions of the brain for each group of patients.

E. Graph theoretical approaches

E.1 Fixed Sparsity Threshold

Anatomical cortical networks for each group were represented by binarized matrix A_{ij} with *N* nodes and *K* edges, where the *N* nodes represent the 68 distinct cortical regions of the brain and the *K* edges represent the corresponding non-zero elements of between the cortical regions. To overcome the issue of differences in number of edges in distinct graphs and for group comparison studies to reflect the changes due to alternations in topological organization, we used a fixed sparsity to threshold network graphs for both the groups[5, 9]

E. 2 Small-world Analysis

Mean clustering coefficient (C_p) is defined as the average of the clustering coefficient of each node, where the clustering coefficient of each node i (C_i) is the ratio of number of existing connections among the immediately connected neighbors of the node to the total number of all their possible connections. C_p is often regarded as an excellent measure of the local cliquishness or the local efficiency of information transfer for a given network [9]. The average path length (L_p) of the network is defined as the average of the path length over all nodes in the network, where the path length of single node *i* is defined as the total shortest absolute path lengths between node I and all other nodes divided by *N*-1. A shorter path length L_p may be indicator of higher global efficiency of the network for information flow.

E.3 Nodal Centrality

Betweenness centrality is used to investigate the nodal characteristics of the *ACM*s among the ApoE4 carriers and non-carriers. Betweenness (B_i) of a node *i* is defined as the number of shortest paths between any two nodes that run through the node *i*. For comparison across groups, the normalized betweenness defined as $b_i = B_i/B$, where B is the average betweenness of all the nodes of the network. Nodal centrality based on betweenness enables us to demark nodes of the cortical brain networks as hubs with $B_i \geq 1.5B$[5].

III. Results

A. Interregional Correlations

Fisher's Z transformation used to reveal significant ($p < 0.05$, FDR-corrected) between-group differences in pairs of cortical regions between the ApoE4 non-carriers and carriers. Cortical region pairs which show significant differences are

listed in Table 1. It is seen that for the four cortical region pairs found significantly different among the two groups, the interregional correlations are positively higher in ApoE4 carriers as compared to ApoE4 non-carriers.

Table 1: Abnormal cortical correlations in ApoE4 carriers and ApoE4 non-carriers.

Region	Region	Correlation, r ApoE4 Non-carrier	ApoE4 Carrier	Z Score
1. L precentral	R superior frontal	0.30	0.60	-2.03
2. R caudal anterior cingulate	R temporal	-0.29	0.49	-4.37
3. R lateral occipital	R lingual	0.28	0.59	-2.09
4. R postcentral	R supra-marginal	0.28	0.59	-2.08

Figure 2 shows that most of the short length connections (Euclidean distance between nodes D< 75mm [5, 10]) are found in the posterior cortex, mainly in the parietal and occipital lobes of the brain for both groups. However, ApoE4 carriers show a reduced amount of short connections in the frontal lobe as compared to non-carriers. Also, long range connections (D >75 mm) are found more prevalent in the parietal and temporal lobes for both groups, but for ApoE4 carriers they do show increased presence in the frontal lobe.

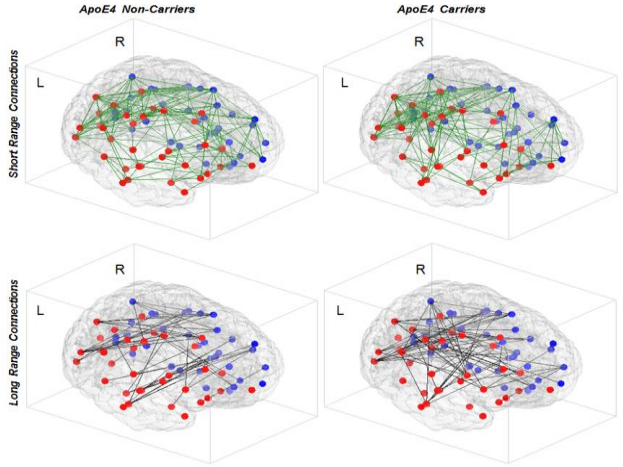

Figure 2: Anatomical representation of the short range (top row) and long range (bottom row) cortical connections in ApoE4 carriers (right column) and non-carriers (left column).

B. *Small-world Properties of Cortical Networks*

In the present study the examination of the small-world properties of the anatomical networks revealed that the networks for both ApoE4 non-carriers and carriers demonstrated small-world architecture with path lengths similar to those of matched random networks ($\lambda \sim 1$) but were more locally clustered ($\gamma > 1$) for a wide range of sparsity from $0.2 \leq S \leq 0.5$.

In order to examine if these changes were related to the differences in genotype between the two groups, Figure 3 presents the mean clustering coefficient and characteristic path length of the networks as a function of the sparsity. Over the range of sparsity studied ($0.2 \leq S \leq 0.5$), ApoE4 carriers demonstrated a higher mean clustering coefficient and longer characteristic path lengths as compared to non-carriers. These results imply that small world properties were altered in the structural networks as a function of cortical thickness.

C. *Hub Regions*

Normalized betweenness was used to determine regions of the cortical network that act as hubs with increased connectivity. Table 2 lists the regions of the brain that are identified as hubs in the anatomical cortical thickness based connectivity analysis for both carriers and non-carriers.

It is seen from Table 2, that a majority of the hub regions for both ApoE4 non-carriers and carriers are located in the frontal and temporal regions. This is also seen in MCI patients where hub regions are found to be located primarily in the temporal and frontal regions. It is also observed that ApoE4 non-carriers show a higher number of hubs as compared to ApoE4 carriers. Hubs appear to be distributed similarly among the hemispheres, with an approximately equal number of hubs seen on both hemispheres. Interestingly, analogous region of the left hemisphere, namely Caudal middle frontal, fusiform, lateral orbitofrontal, pars triangularis and insula, are seen as hub regions in both ApoE4 non-carriers and carriers; something not seen in the right hemisphere, except for the fusiform region.

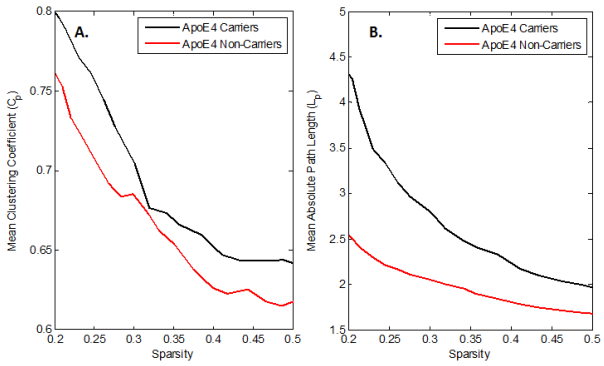

Figure 3: Mean clustering coefficients and mean path lengths are plotted as a function of sparsity ranging from 0.2 to 0.5 for both ApoE4 carriers (black) and non-carriers (red). The mean clustering coefficient and the mean absolute path lengths were found to be larger in the ApoE4 carriers.

Table 2: Hub regions identified in the anatomical cortical networks for ApoE4 non-carriers and carriers

ApoE4 Non-Carriers		ApoE4 Carriers	
Left Hemisphere			
Region	Lobe*	Region	Lobe*
Caudal middle frontal	F	Caudal middle frontal	F
Lateral orbitofrontal	F	Lateral orbitofrontal	F
Pars triangularis	F	Pars orbitalis	F
Rostral anterior cingulate	F	Pars triangularis	F
Rostral middle frontal	F	Insula	I/T
Superior frontal	F	Pericalcarine	O
Insula	I/T	Precuneus	P
Supramarginal	P	Fusiform	T
Fusiform	T	Temporal pole	T
Middle temporal	T		
Superior temporal	T		
Right Hemisphere			
Region	Lobe	Region	Lobe
Caudal middle frontal	F	Caudal anterior cingulate	F
Pars triangularis	F	Cuneus	O
Rostral middle frontal	F	Lingual	O
Superiorfrontal	F	Posterior cingulate	P
Posterior cingulate	P	Entorhinal	T
Fusiform	T	Fusiform	T
Middle temporal	T	Inferior temporal	T
Parahippocampal	T		

*F = Frontal, T= Temporal, P =Parietal, O = Occipital and I = Insula

IV. Discussion

This study used interregional correlation coefficients among cortical thicknesses to evaluate large-scale and small world properties of anatomical networks for ApoE4 carriers and non-carriers. The main findings of this study demonstrates that (1) both ApoE4 carriers and non-carriers demonstrated small-world properties; (2) Abnormal nodal characteristics as measured by clustering coefficient, path lengths and node betweenness was observed in ApoE4 carriers as compared to ApoE4 non-carriers; (3) The interregional correlation coefficients showed significant differences between the ApoE4 carriers and non-carriers. These findings in ApoE4 carriers, who are at a higher risk of developing AD, show that structural imaging based evidence can point to alterations in the coordination of large-scale brain networks.

AD subjects have been reported to display decreased positive correlation among bilaterally symmetric parietal regions [5, 10]. In this study based in control subjects we did not see significant changes in bilaterally symmetric regions of the brain in ApoE4 carriers. This suggests that ApoE4 carriers although at a higher risk do not display the loss of coordination in bilaterally symmetric regions, which is characteristic of AD patients, and may be attributed to later stages of the disease.

The hub regions found in the study are consistent with previous studies reported in normal controls which showed an increased localization in the temporal and frontal lobes, primarily aligned with the default mode network (DMN) of the brain [11]. The study found that regions of the DMN like middle temporal gyrus, para-hippocampal cortex, posterior cingulate, and precuneus are seen across the sub-groups, but are organized differently among the groups. ApoE4 non-carriers demonstrated higher betweenness in regions such as middle temporal, para-hippocampal gyrus, posterior cingulate and insula which have been demonstrated to be involved in memory and integration [12]. The loss of these hubs in ApoE4 carriers can be related to early deactivation of core areas of the DMN seen in AD and also pre-symptomatic individuals with a higher risk of AD susceptibility[13]. The lack of connectivity in the DMN primarily in the para-hippocampal gyrus among ApoE4 carriers has also been shown in pre-symptomatic individuals in visual coding tasks through fMRI imaging [14]. Also, ApoE4 is related to higher $A\beta$ deposition in PiB findings as well as lower $A\beta$1-42 CSF concentrations in non-demented individuals [6].

To the best of our knowledge this is the first study to demonstrate results consistent with these functional studies using only structural measures (cortical thickness). We demonstrated that the hubs of structural connectivity as seen through MR imaging in regions like para-hippocampus and middle temporal of the medial temporal lobe (MTL) and the DMN are lost in ApoE4 carriers.

Results demonstrated rather similar distribution of hubs in the left hemisphere for both carriers and non-carrier, which was not seen in the right hemisphere. This finding is in alignment with various studies which have demonstrated an asymmetric distribution of morphological features across hemispheres for patients with MCI and AD[15].

In addition to the regions of the brain that show loss of connectivity in ApoE4 carriers as demonstrated by loss of hubs, some regions of the brain also show an increase in the nodal betweenness and appear as new hubs as compared to non-carriers. Such increase is often addressed as a compensatory system of the brain. This compensatory increase in connectivity in core regions of the brain may play an important role in enabling patients to use additional cognitive resources to approach a normal level [5, 10]. Moreover, APoE4 carriers showed a larger number of long length connections and a reduction in number of short length connections as compared to non-carriers. We speculate that this alternate distribution of the networks connections may be contributing to the compensatory mechanism.

References

[1] T. Koenig, L. Prichep, T. Dierks, D. Hubl, L. O. Wahlund, E. R. John, *et al.*, "Decreased EEG synchronization in Alzheimer's disease and mild cognitive impairment," *Neurobiol Aging,* vol. 26, pp. 165-71, Feb 2005.

[2] C. J. Stam, B. F. Jones, I. Manshanden, A. M. van Cappellen van Walsum, T. Montez, J. P. Verbunt, *et al.*, "Magnetoencephalographic evaluation of resting-state functional connectivity in Alzheimer's disease," *Neuroimage,* vol. 32, pp. 1335-44, Sep 2006.

[3] J. Wang, L. Wang, Y. Zang, H. Yang, H. Tang, Q. Gong, *et al.*, "Parcellation-dependent small-world brain functional networks: a resting-state fMRI study," *Hum Brain Mapp,* vol. 30, pp. 1511-23, May 2009.

[4] G. L. Gong, Y. He, L. Concha, C. Lebel, D. W. Gross, A. C. Evans, *et al.*, "Mapping Anatomical Connectivity Patterns of Human Cerebral Cortex Using In Vivo Diffusion Tensor Imaging Tractography," *Cerebral Cortex,* vol. 19, pp. 524-536, Mar 2009.

[5] Y. He, Z. Chen, and A. Evans, "Structural insights into aberrant topological patterns of large-scale cortical networks in Alzheimer's Disease," *Journal of Neuroscience,* vol. 28, pp. 4756-4766, 2008.

[6] D. A. Wolk, B. C. Dickerson, and A. s. D. Neuroimaging, "Apolipoprotein E (APOE) genotype has dissociable effects on memory and attentional-executive network function in Alzheimer's disease," *Proceedings of the National Academy of Sciences of the United States of America,* vol. 107, pp. 10256-10261, Jun 1 2010.

[7] D. J. Watts and S. H. Strogatz, "Collective dynamics of 'small-world' networks," *Nature,* vol. 393, pp. 440-442, Jun 4 1998.

[8] R. S. Desikan, F. Segonne, B. Fischl, B. T. Quinn, B. C. Dickerson, D. Blacker, *et al.*, "An automated labeling system for subdividing the human cerebral cortex on MRI scans into gyral based regions of interest," *Neuroimage,* vol. 31, pp. 968-980, Jul 1 2006.

[9] S. Achard and E. Bullmore, "Efficiency and cost of economical brain functional networks," *PLoS Comput Biol,* vol. 3, p. e17, Feb 2 2007.

[10] Z. Yao, Y. Zhang, L. Lin, Y. Zhou, C. Xu, T. Jiang, *et al.*, "Abnormal cortical networks in mild cognitive impairment and Alzheimer's disease," *PLoS Comput Biol,* vol. 6, p. e1001006, 2010.

[11] D. A. Fair, A. L. Cohen, N. U. Dosenbach, J. A. Church, F. M. Miezin, D. M. Barch, *et al.*, "The maturing architecture of the brain's default network," *Proc Natl Acad Sci,* vol. 105, pp. 4028-32, 2008.

[12] H. Oh and W. J. Jagust, "Frontotemporal Network Connectivity during Memory Encoding Is Increased with Aging and Disrupted by Beta-Amyloid," *Journal of Neuroscience,* vol. 33, pp. 18425-18437, Nov 20 2013.

[13] C. Pena-Gomez, C. Sole-Padulles, I. C. Clemente, C. Junque, N. Bargallo, B. Bosch, *et al.*, "APOE status modulates the changes in network connectivity induced by brain stimulation in non-demented elders," *PLoS One,* vol. 7, p. e51833, 2012.

[14] Z. Liu, Y. Zhang, H. Yan, L. Bai, R. Dai, W. Wei, *et al.*, "Altered topological patterns of brain networks in mild cognitive impairment and Alzheimer's disease: a resting-state fMRI study," *Psychiatry Res,* vol. 202, pp. 118-25, May 31 2012.

[15] Q. Zhou, M. Goryawala, M. Cabrerizo, W. Barker, R. Duara, and M. Adjouadi, "Significance of normalization on anatomical MRI measures in predicting Alzheimer's disease," *ScientificWorldJournal,* vol. 2014, p. 541802, 2014.